Corrosion inhibition of 2024 aluminium alloy by sodium decanoate

Grégory Boisier, Nicolas Portail, Nadine Pébère *,[1]

Université de Toulouse, CIRIMAT, UPS/INPT/CNRS, ENSIACET, 118 route de Narbonne, 31077 Toulouse Cedex 04, France

A B S T R A C T

The present study concerns the corrosion protection of the aluminium alloy (AA) 2024 by sodium decanoate (a long-carbon-chain carboxylate). This compound-type is known to form hydrophobic films on the metal surface. The characterization of the inhibition mechanisms was studied for different experimental conditions (pH, NaCl concentrations) by using electrochemical techniques. Special attention was paid to the action of the carboxylate on the intermetallic particles by performing local electrochemical impedance measurements on a model system (Al/Cu couple). The decanoate afforded high protection to the AA2024 both by preventing chloride ion attack of the oxide layer and by limiting galvanic coupling between the intermetallic particles and the surrounding matrix. A passivation effect of the compound was also shown.

Keywords:
Aluminium alloy
Carboxylates
Inhibition
Intermetallics
Impedance

1. Introduction

In the aeronautic industry, the corrosion protection of structural aluminium alloys, such as the 2XXX series requires different surface treatments which involve the use of Cr(VI) to obtain high corrosion resistance. One of the main actions of chromates, which explains their efficiency, is their self-repairing effect. Their strong oxidising power stops corrosion by forming a new and efficient passive layer on the Al alloy surface [1–4]. Since the beginning of the 1990s, the high toxicity associated with chromates has imposed restrictions on their use in industrial applications. As a consequence, intense research efforts are being undertaken to find new environmentally friendly compounds as corrosion inhibitors of aluminium alloys. In the case of AA2024, it has been established that very small amounts of copper in the aluminium affect its corrosion resistance. The presence of alloying elements and hence noble phases in the microstructure produces local electrochemical cells which lead to the breakdown of the oxide film and to corrosive attack in aggressive environments [5–17].

Among the numerous studies concerning the replacement of Cr(VI), some compounds such as rare earth salts [18–24] or organic compounds [25,26] have presented interesting corrosion protection activity. However, despite the promising performances, these compounds do not offer the same level of protection as chromates, particularly in surface treatments. In a recent study, we used long-carbon-chain carboxylic acids (CH_3–$(CH_2)_n$–COOH) for the post-treatment of hydrothermally sealed AA2024 anodic layers formed in tartaric–sulphuric acid [27]. It was shown that the formation of the aluminium soap conferred hydrophobic properties to the surface and thus provided a protective action which was clearly revealed by a significant enhancement of salt spray test resistance compared to untreated specimens. Monocarboxylic acids are environmentally friendly and are known to act as corrosion inhibitors for various metals such as copper [28], lead [29], mild steel [30–32] aluminium alloys [33], and magnesium alloys [34]. The hydrophobic characteristics of monocarboxylic acids depend strongly on their carbon chain length [31–34]. In aqueous solution, the carboxylic group (negatively charged) reacts with the metal surface (positively charged [35,36]) to form carboxylate bonds. In spite of these interesting properties, few works have been devoted to the use of carboxylic acids for corrosion protection of AA2024.

The present paper focuses on the use of the sodium salt of a linear carboxylic acid as corrosion inhibitor of AA2024. As a trade off between solubility, which decreases as the carbon chain length increases, and the efficiency, the compound which was selected was the sodium decanoate (CH_3–$(CH_2)_8$–COONa). The efficiency and the corrosion mechanisms were investigated by using stationary electrochemical techniques, conventional and local electrochemical impedance spectroscopy (EIS) and contact angle measurements. First, the film formation and the influence of the aggressiveness of the electrolyte (pH, NaCl concentration) on the corrosion resistance of the AA2024 were investigated. Then, to show the inhibitive action of the molecules on the intermetallic

* Corresponding author. Tel.: +33 5 62 88 56 65; fax: +33 5 62 88 56 63.
E-mail address: Nadine.Pebere@ensiacet.fr (N. Pébère).
[1] ISE member.

doi:10.1016/j.electacta.2009.10.080

particles, a Al/Cu model couple was used. Finally, the protective properties of the carboxylate were evaluated and compared to those of a cerium salt.

2. Experimental

2.1. Materials

The decanoic acid and the cerium nitrate, purchased from Merck, were used as received. The corrosive medium was prepared from distilled water by adding 0.1 M Na_2SO_4 (reagent grade). Sodium decanoate was obtained by neutralisation of the decanoic acid with a 0.5 M sodium hydroxide solution. The sodium decanoate concentration was fixed at 0.05 M which provides the highest inhibition efficiency (previously determined from electrochemical measurements) and corresponds to the solubility limit of the compound. For specific experiments, the pH of the solution was adjusted (4, 6, 8 or 10) by sodium hydroxide (0.5 M solution) or by sulphuric acid (0.5 M solution). NaCl was added to the Na_2SO_4 solution at different concentrations. The electrolytic solution was in contact with air at 25 °C. For the local impedance experiments with the Al/Cu model couple, the solutions were more diluted and were composed, either of 0.05 M sodium decanoate or 0.001 M Na_2SO_4.

Aluminium alloy 2024 T351 was used for the investigations. The average chemical composition of the alloy is given in Table 1. The T351 temper corresponds to a heat treatment conducted at 495 °C (±5 °C), water quenching, straining and tempering at room temperature for 4 days. Electrochemical experiments were carried out on an AA2024 T351 rod of 1 cm^2 cross-sectional area machined from a rolled plate (cylinder surface parallel to the plane of rolling). The body of the rod was covered with a heat-shrinkable sheath, leaving only the tip of the sample cylinder in contact with the solution. The samples were polished with SiC paper down to grade 4000, successively rinsed with permuted water, acetone, and ethanol and finally dried in warm air.

In order to study the interactions between the sodium decanoate and the intermetallic particles, a simple system consisting of a pure aluminium/pure copper (Al/Cu) couple was used. This model couple was designed to study the corrosion phenomena associated with copper-rich intermetallics in aluminium alloys in a previous investigation [37]. The electrode was prepared as follows: a cylinder of pure aluminium (99.999 wt.%) was drilled in its centre and a cylinder of pure copper (99.9 wt.%) was introduced by force into the hole (Fig. 1). The assembly of the two materials gave a perfectly joined interface, avoiding any crevice corrosion due to surface defects. The radii were 1 and 0.32 cm for the aluminium and copper bars, respectively. The electrode was then embedded in an epoxy resin. Before immersion in the electrolyte, the Al/Cu disk electrode was prepared in the same way as the AA2024 rod.

2.2. Contact angle measurements

The contact angles were measured using a Digidrop Contact Angle Meter from GBX Scientific Instruments. The protocol used consists in depositing a liquid drop of an accurately known volume (3–5 μL) on the surface of the sample and then measuring the static contact angle (θ). In the present study, a few seconds were sufficient to obtain stabilization of the interfacial forces and thus, the static contact angle was measured just after deposition of the liquid drop. In order to assess the homogeneity of the surface properties, 20 measurements were performed at different locations on the samples and the average contact angle was calculated. Deionised water was used as the liquid for the droplets to evaluate the hydrophilic ($\theta < 90°$) or hydrophobic ($\theta > 90°$) character of the surface. All the experiments were performed at room temperature and constant humidity (~50%).

Table 1
Chemical composition (wt.%) of 2024 T351 aluminium alloy.

Cu	4.50
Mg	1.44
Mn	0.60
Si	0.06
Fe	0.13
Zn	0.02
Ti	0.03
Al	Bal.

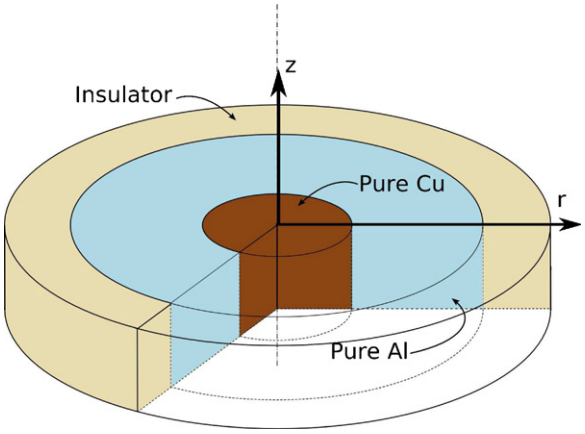

Fig. 1. Schematic representation of the pure Al/pure Cu model couple.

2.3. Electrochemical measurements

For the conventional experiments, a three-electrode cell was used with a platinum grid auxiliary electrode, a saturated calomel reference electrode (SCE) and the rod of AA2024 as rotating disk electrode. The rotation rate was fixed at 500 rpm. Polarisation curves were plotted under potentiodynamic regulation using a Solartron 1287 electrochemical interface. The anodic and the cathodic parts were obtained independently from the corrosion potential at a potential sweep rate of 1 V h^{-1}. Electrochemical impedance measurements were carried out at the corrosion potential using a Solartron 1287 electrochemical interface connected with a Solartron 1250 frequency response analyser. Impedance diagrams were obtained over a frequency range of 65 kHz to a few mHz with six points per decade using a 20 mV peak-to-peak sinusoidal potential. The electrochemical results were obtained from at least three experiments to ensure reproducibility.

The corrosion behaviour of the model couple with and without sodium decanoate was studied by local electrochemical impedance spectroscopy (LEIS). The measurements were carried out with a Solartron 1275 system. This method used a five-electrode configuration [38–40]. The probe (i.e., a bi-electrode allowing local current density measurement) was stepped across a selected area of the sample. The analyzed part had an area of 12 mm × 12 mm (24 mm × 24 mm for the experiment without inhibitor) and the step size was 500 μm in the X and Y directions. Admittance was plotted rather than impedance to improve the visualization of the mapping. The maps were obtained at fixed frequencies chosen in the present case at 1 kHz and 1 Hz. The local impedance measurements were carried out in a low conductivity medium to optimize resolution. With the experimental set up used, only the normal component of the current was measured.

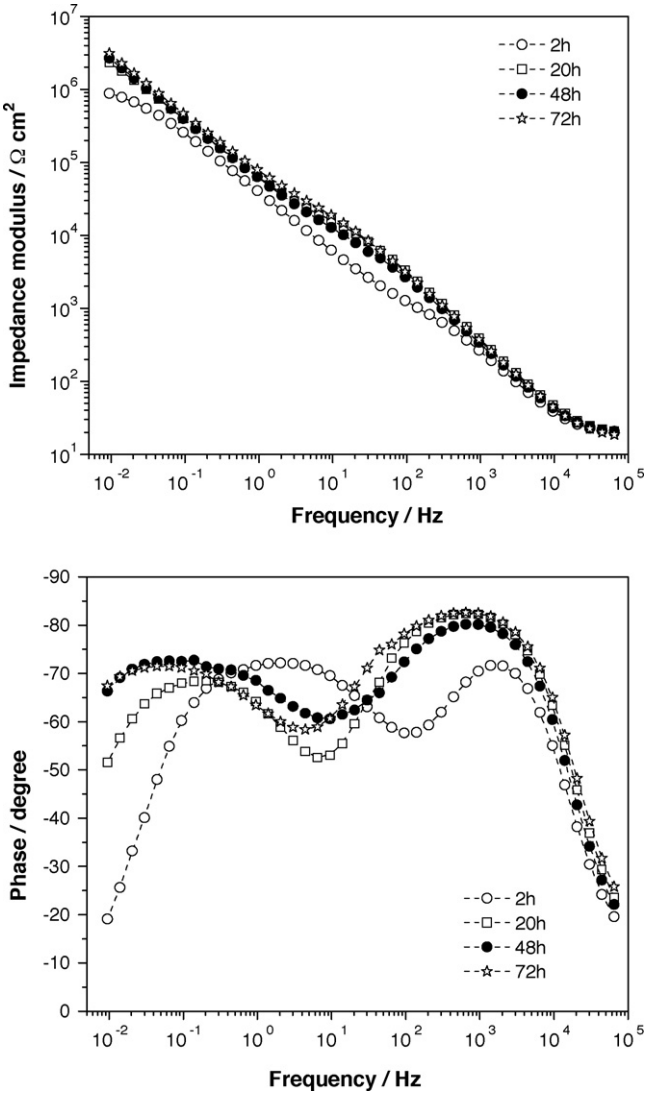

Fig. 2. Impedance diagrams obtained on the AA2024 at the corrosion potential after different immersion times in a solution containing 0.1 M Na_2SO_4 + 0.05 M NaCl + 0.05 M sodium decanoate (pH 6).

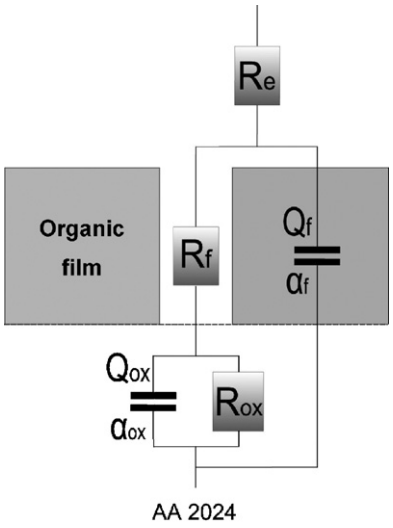

Fig. 3. Equivalent electrical circuit used to model the impedance diagrams on AA2024 in the presence of sodium decanoate (R_e: electrolyte resistance; R_f: resistance of the solution in the pores of the organic film; Q_f and α_f: parameters associated to the properties of the organic film; R_{ox}: resistance associated to the oxide film; Q_{ox} and α_{ox}: parameters associated to the properties of the oxide film).

3. Results and discussion

3.1. Characterization of the growth of the organic film on the AA2024 surface

Electrochemical impedance diagrams were plotted versus immersion time in the electrolytic solution containing sodium decanoate (0.05 M). Independently of the immersion time, the diagrams are characterized by two time constants (Fig. 2). The first in the high frequency range was attributed to the presence of an organic film while the oxide layer/organic film interface was characterized in the low-frequency range. These observations allowed an electrical equivalent circuit to be proposed (Fig. 3). The two parts of the circuit were imbricated to follow the hypothesis of the presence of zones not covered by the organic molecules or, in other words, where the presence of the molecules decreases the active surface in contact with the electrolyte. This equivalent circuit is similar to that often use to describe the behaviour of organic coatings [41,42]. Parameters α and Q introduced into the equivalent circuit are associated to a constant phase element (CPE) to take into account the non-ideal behaviour of the interface [40]. The experimental diagrams are perfectly fitted with the equivalent circuit and thus the values of the parameters can be extracted. Fig. 4 presents the variations of R_f, R_{ox}, Q_f and Q_{ox} obtained from the fitting of the experimental data. After 2 h of immersion, the value of R_f is high (2.3 kΩ cm^2) indicating the formation of a dense organic film on the alloy surface. The variation of R_f with time indicates that the film no longer changes after 20 h of immersion. In contrast, R_{ox} continues to increase for the 72 h of immersion. The R_{ox} measurement is sensitive to the variation of the surface area (the only low-frequency current sources). Since the pores of the film represent the bare part of the surface (oxide-covered metal), the increase of R_{ox} after 20 h of immersion can be explained by a decrease of the number of pores probably due to local molecule rearrangements to minimise interfacial energy. Q_f and Q_{ox} decreased slowly with immersion time which corroborates the strengthening of the organic film. α_f and α_{ox} were about 0.9 and 0.8, respectively. The value of α_{ox} is in agreement with the value previously obtained on pure Al and the constant phase element behaviour has been attributed to 3D heterogeneity of the aluminium oxide layer [40].

In the literature, the corrosion protection afforded by carboxylates, when the carbon chain is long enough, has been explained by the hydrophobic character of the film which strongly decreases the surface wettability [43]. The inhibitive organic film is water repellent and impedes the aggressive species from reaching the metal surface. It was seen from the electrochemical measurements that an organic film was formed on the alloy surface and thus it is interesting to study the influence of its growth on the hydrophobic properties of the surface. Contact angle measurements were performed on different samples treated in a solution containing 0.1 M Na_2SO_4 + 0.05 M sodium decanoate after different immersion times. The results are reported in Fig. 5. Before immersion, the surface shows a hydrophilic character with a contact angle of around 30°. After 1 min of immersion in the solution, the contact angle was 115° revealing the hydrophobic character of the surface. Then, no variation of the hydrophobic character of the surface occurred with the immersion time. Nevertheless, it can be noted that less than 1 min was necessary to obtain a hydrophobic film. The contact angle measurements revealed that the decanoate molecules were rapidly and strongly adsorbed to the alloy surface. However,

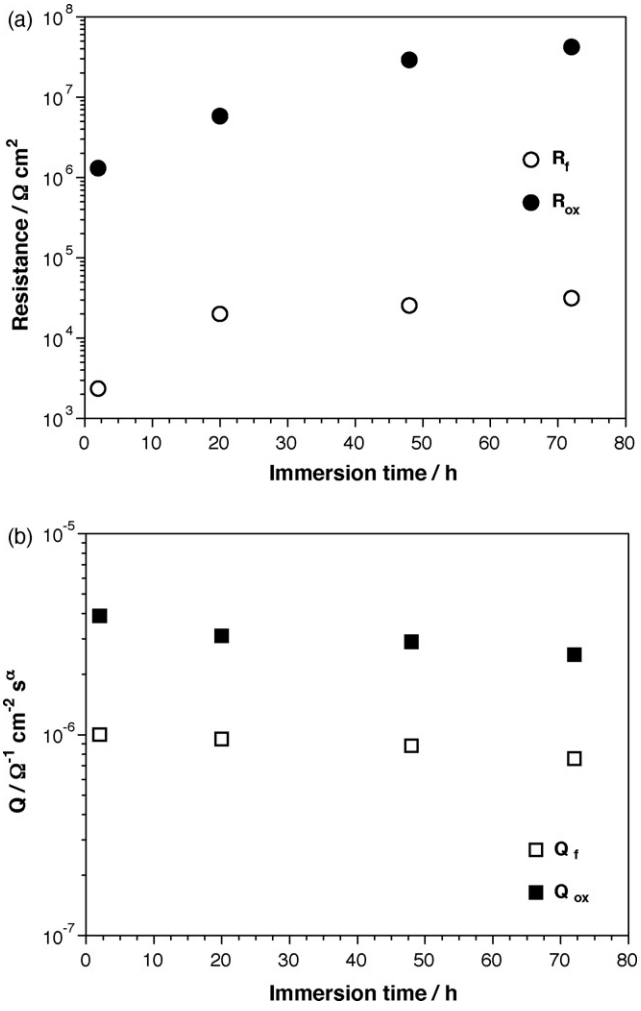

Fig. 4. (a) R_f and R_{ox} and (b) Q_f and Q_{ox} versus immersion time in a solution containing 0.1 M Na_2SO_4 + 0.05 M NaCl + 0.05 M sodium decanoate (pH 6).

the measurements are relatively macroscopic (the water drop has a diameter of about 1 mm), and thus, the local re-arrangements which are assumed to occur for longer immersion times (t > 1 min) cannot be shown by the technique.

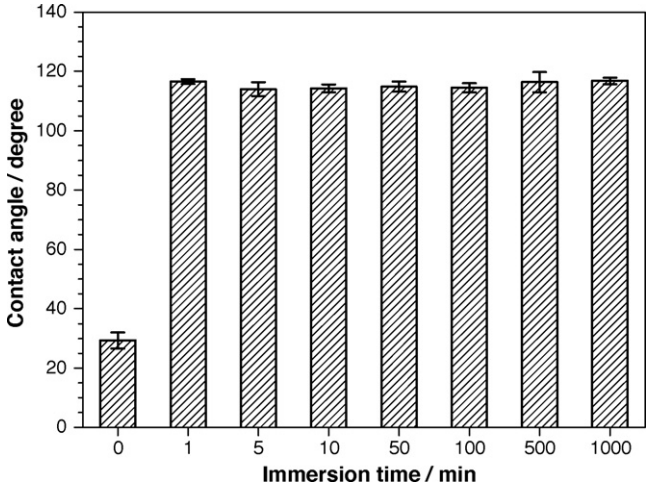

Fig. 5. Contact angles measured on the AA2024 after different exposure times to a solution containing 0.1 M Na_2SO_4 + 0.05 M sodium decanoate (pH 6).

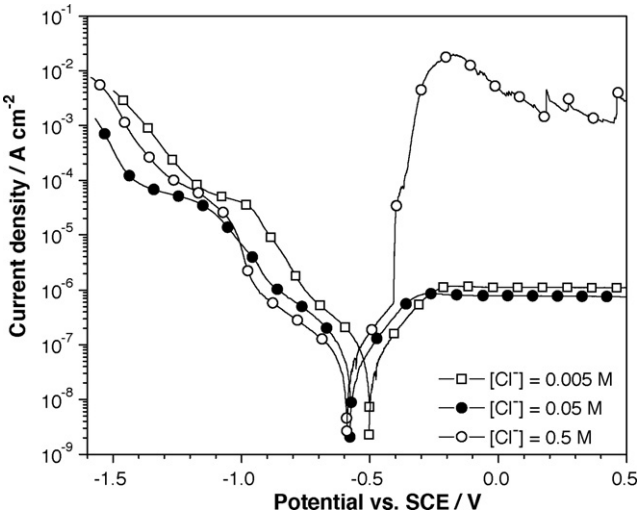

Fig. 6. Polarisation curves obtained on the AA2024 after 2 h of immersion in a solution containing 0.1 M Na_2SO_4 + 0.05 M sodium decanoate with different NaCl concentrations (pH 6).

3.2. Characterization of the corrosion resistance

Polarisation curves of the AA2024 were plotted in a solution containing 0.1 M Na_2SO_4 + 0.05 M sodium decanoate and different NaCl concentrations (0.005, 0.05 and 0.5 M). The curves are shown in Fig. 6. The cathodic parts and the anodic current densities around the corrosion potential were similar for the three concentrations. This explains that the impedance diagrams plotted at the corrosion potential for the three concentrations were identical (not reported). The corrosion potential was slightly shifted towards cathodic potentials as the NaCl concentration increased; in the absence of inhibitors (the curves are not reported here), the corrosion potential was strongly dependent on the NaCl concentration. The greatest modification on the polarisation curves concerned the pitting potential, which results from the breakdown of the passive film. Whereas for the lowest NaCl concentrations (0.005 and 0.05 M), a large passivity plateau can be observed until 1 V/SCE, a higher chloride concentration (0.5 M) led to the breakdown of the passive film for an overpotential of about 200 mV. The length of the passivity plateau was reduced and thus the probability of pitting at the corrosion potential was increased. The stability of E_{corr}, as the NaCl concentration increased, and the large passivity plateau observed, indicate the significant barrier effect played by the organic film in repelling the Cl^- ions. For the highest NaCl concentration, we can assume that a sufficient quantity of Cl^- can reach the AA2024 surface enabling the passive layer to be attacked. As for different inhibitive species, such as chromates [44], the ratio [Cl^-]/[carboxylates] must be kept low to optimize efficiency.

The ability of the inhibitor to form a protective film on AA2024 was investigated over a large pH range (4, 6, 8 and 10). The impedance diagrams obtained after 2 h of immersion are presented in Fig. 7. Independently of the pH, the diagrams were always characterized by two time constants and can be fitted by the equivalent circuit presented in Fig. 3. The parameters obtained from the fitting of the experimental curves are given in Table 2. It must be emphasized that the pH modifies the inhibitive species. The pK_a of the decanoic acid/decanoate couple is 4.84. For pH values higher than 4.84, the predominant form in solution is the decanoate anion whereas for lower pH values, the decanoic acid is the predominant species in solution. Thus, for pH values close to the pK_a, the decanoate concentration in the electrolyte can decrease. This was confirmed during the preparation of the solution

Table 2
Fitted values of the parameters associated to the impedance diagrams obtained for the AA2024 after 2 h of immersion in a solution containing 0.1 M Na_2SO_4 + 0.05 M sodium decanoate at different values of the pH.

pH	$R_e/\Omega\,cm^2$	$R_f/k\Omega\,cm^2$	$Q_f/\mu\Omega^{-1}\,cm^{-2}\,s^{\alpha}$	α_f	$R_{ox}/k\Omega\,cm^2$	$Q_{ox}/\mu\Omega^{-1}\,cm^{-2}\,s^{\alpha}$	α_{ox}
4	13	10	1.2	0.83	460	3.5	0.69
6	11	4.6	1.4	0.92	705	5.8	0.80
8	16	3.4	1.4	0.93	750	5.9	0.81
10	13	0.3	4.5	0.86	520	2.1	0.88

at pH 4 where precipitation of decanoic acid occurred. However, a complementary experiment performed at a lower decanoate concentration (0.01 M) showed comparable results indicating that the form of the inhibitive species has little effect on the electrochemical results. The analysis of the values reported in Table 2 shows a variation of the film resistance (R_f) versus pH. The value of R_f was maximum for a pH of 4 and minimum for a pH of 10. To explain these observations, the surface charge of the aluminium must be also taken into account. At pH 4, the surface is positively charged and the alloy dissolved preferentially in the form of Al^{3+}. Thus, film formation *via* the negatively charged decanoate anions was favoured explaining the high value of R_f. Nevertheless, acidity of the solution contributed, by dissolution of the passive layer, to the decrease of R_{ox}, which was slightly lower than for the other pH values. At pH 6 and 8, the aluminium was protected by the oxide layer and, since the pH values were less than the isoelectric point of oxide-covered aluminium which is 9.5 [35,36], the surface acquired a positive charge favouring film formation. It is also possible that a preliminary step of metal oxidation was necessary for the precipitation of the organic film [28,34]. The organic film was assumed to be homogeneous explaining that the value of R_{ox} was higher for these two pH values. The results obtained at pH 6 and 8 were identical and show that the efficiency of the inhibitor was constant in a pH range where the alloy was in the passive state. For a pH of 10, greater than the isoelectric point, the surface became negatively charged and the alloy dissolved by forming AlO^{2-} ions. The presence of the negative charges induced electrostatic repulsion with the decanoate which was then unable to interact strongly with the surface. This explains why the value of R_f was low. In addition, the increase of the free surface area, linked to the fact that the organic film did not cover the surface correctly, was responsible for the decrease of R_{ox}.

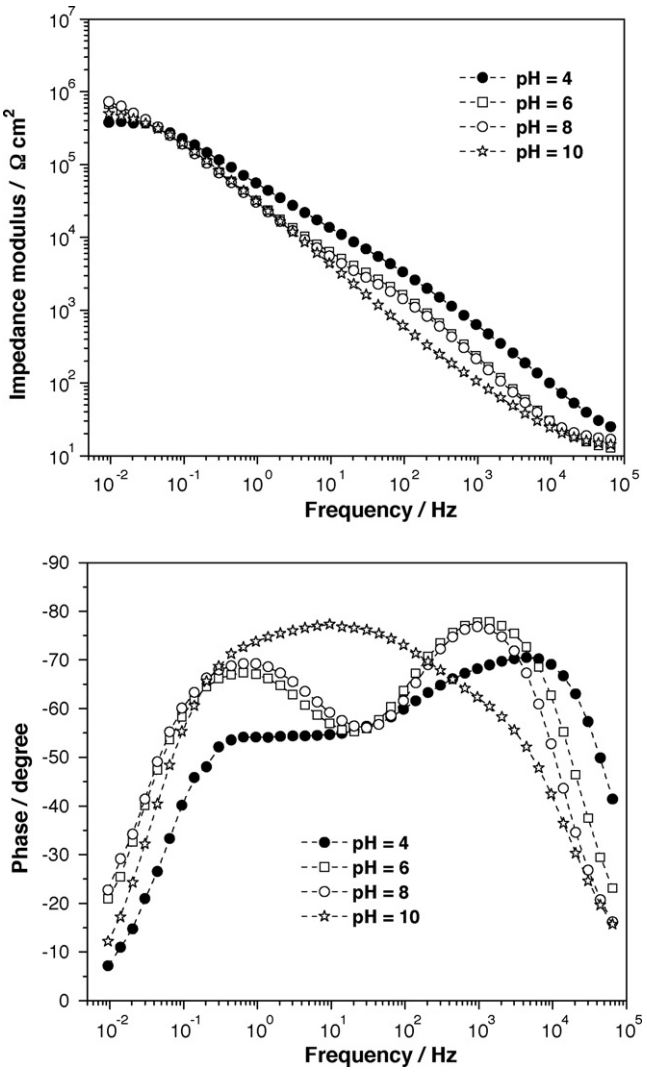

Fig. 7. Impedance diagrams obtained on the AA2024 at the corrosion potential after 2 h of immersion in a solution containing 0.1 M Na_2SO_4 + 0.05 M NaCl at different pH values.

In spite of the observed differences, both the R_f and R_{ox} values were high showing the efficiency of the sodium decanoate in the studied pH range.

3.3. Interactions of the decanoate with the intermetallic particles

The inhibition mechanism of pure metals by carboxylate anions is relatively simple and well described in the literature. The majority of aluminium alloys have heterogeneous microstructures due to the presence of intermetallic particles and thus, it is interesting to carry out local characterization of the action of the decanoate to better understand how the inhibition mechanisms affect these particles. The Al/Cu model couple was immersed in an aqueous solution with 0.05 M decanoate. Maps of the impedance modulus at 1 kHz (characteristic frequency of the presence of the organic film) after 2 and 72 h of immersion are presented in Fig. 8. The results indicate a strong decrease of the admittance modulus between 2 and 72 h of immersion. This variation, which corresponds to an increase of R_f, shows the growth of the organic film at the surface of both materials with the immersion time. After 72 h of immersion, the admittance modulus was higher on the copper electrode (lower resistance) than on the aluminium electrode. The galvanic coupling between the two metals can partly explain the observed difference: in the Al/Cu couple, aluminium is the anode of the system and is in the passive state while copper is polarized cathodically [37]. Thus, on the aluminium electrode, the polarisation imposed by the coupling strengthened the passive layer which is favourable to decanoate adsorption. In contrast, on the copper electrode, the cathodic reduction led to the formation of hydroxyl ions susceptible to induce electrostatic repulsion with the decanoate. Thus, with increasing immersion times, the galvanic coupling will be less favourable on the copper surface to the interactions of decanoate than on aluminium.

LEIS measurements were also performed at 1 Hz (frequency characteristic of the corrosion process) in the presence of decanoate (Fig. 9b) and compared to the map obtained without inhibitor (Fig. 9a). In Fig. 9a, admittance was higher on the copper electrode

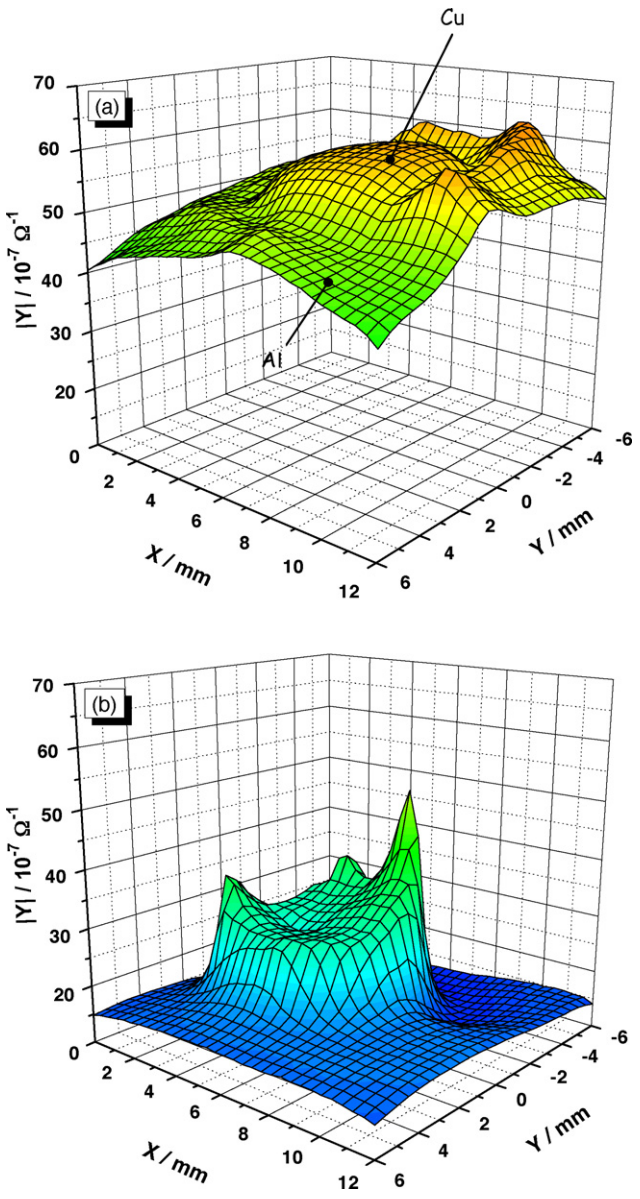

Fig. 8. Local admittance maps on the model couple after (a) 2 h and (b) 72 h of immersion in a solution containing 0.05 M sodium decanoate (pH 6, chloride-free electrolyte). Frequency = 1 kHz.

(lower resistance), attributed to the reduction of oxygen on copper, than on aluminium which is in the passive state [37]. In the presence of decanoate (Fig. 9b), first, it can be noted that the admittance was significantly lower than that obtained without inhibitor. The most significant result is that the impedance modulus is the same on the two parts of the electrode (Cu and Al) showing that the galvanic coupling was negligible and that the organic film protected the whole electrode surface.

From the LEIS results, it can be concluded that the sodium decanoate was adsorbed homogeneously over the Al/Cu electrode, strongly limiting galvanic coupling between the two metals. For AA2024, even though the scale was not the same (4% of copper-rich intermetallic particles instead of 11% of copper in the model couple), it can be assumed that the mechanisms are similar. The presence of copper in the intermetallic particles and the galvanic coupling, mainly responsible for the corrosion of AA2024, do not impede the adsorption of the organic molecules and the efficiency is high.

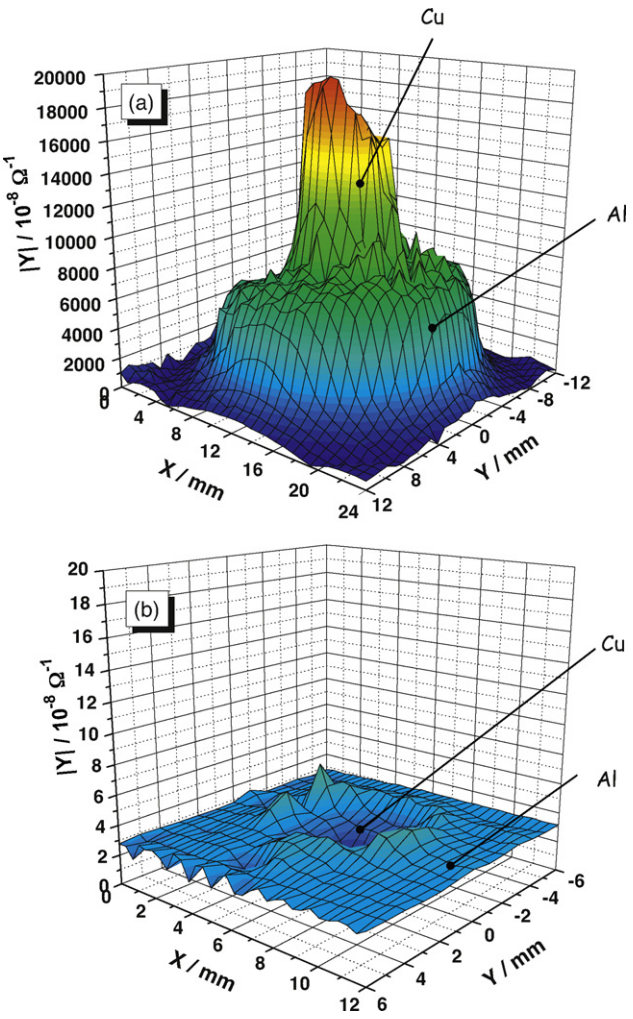

Fig. 9. Local admittance maps on the model couple after 2 h of immersion: (a) without decanoate (0.001 M Na_2SO_4) and (b) in a solution containing 0.05 M sodium decanoate. Frequency = 1 Hz (pH 6, chloride-free electrolyte).

3.4. Protective effect

An important property of corrosion inhibitors is their ability to react with an active surface to stop the corrosion processes. It is well-known that chromates have a pronounced repairing effect (self-healing) [1–4]. To evaluate the ability of sodium decanoate to decrease the corrosion of AA2024, the alloy was polarized anodically at −0.45 V/SCE (overvoltage of 100 mV from E_{corr}) in a solution containing only 0.1 M Na_2SO_4 + 0.05 M NaCl to accelerate the dissolution process. Then, the decanoate was injected into the solution. After decanoate addition, the Na_2SO_4 and the NaCl concentrations were unchanged and the decanoate concentration was 0.025 M (for solubility reasons, the inhibitor concentration cannot reach 0.05 M). During the experiments (3200 s), the anodic current densities were recorded. The results for different inhibitor injection times were shown in Fig. 10. The maximum and the minimum limits of the anodic current densities were obtained for the 0.1 M Na_2SO_4 + 0.05 M NaCl solution with and without inhibitor (Fig. 10). In the absence of the inhibitor, the anodic current density stabilized rapidly at a value of about 4 mA cm^{-2} characterizing the strong dissolution of the metal. In contrast, when the decanoate was present at the beginning of immersion in the aggressive solution, the anodic current density remained very low after 3200 s and reached a value of around 10^{-3} mA cm^{-2} after 3200 s. The curves in Fig. 10 show a significant decrease of the current density

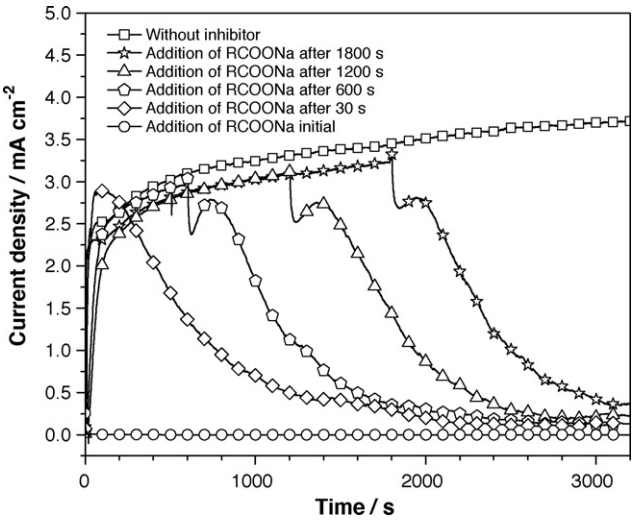

Fig. 10. Anodic current density versus time for the AA2024 polarized at −0.45 V/SCE in a solution containing 0.1 M Na_2SO_4 + 0.05 M NaCl with or without 0.025 M sodium decanoate after different inhibitor injection times (pH 6).

independently of the time at which the decanoate was added to the aggressive solution. The current density decreased, from 4 to 0.1 mA cm^{-2}, showing the protective effect of the decanoate. However, the anodic current densities never reached 10^{-3} mA cm^{-2}, obtained when the inhibitor was initially added to the aggressive solution. The decanoate did not allow the complete passivation of the surface but strongly limited the evolution of the dissolution imposed by the anodic polarisation. Moreover, it can be seen in Fig. 10 that a short time is necessary for the inhibitor to act on the alloy surface. This "protection time" was unaffected by the injection time, remaining between 100 and 150 s. This indicates that the inhibition kinetics was independent of the degradation state of the surface when the inhibitor was injected into the solution.

Identical measurements were performed with cerium nitrate. Fig. 11 compares the curves obtained after injection of the cerium or the decanoate salts after 600 s of polarisation. No significant decrease of the current density was observed with the cerium salt and the curve is similar to that obtained without inhibitor.

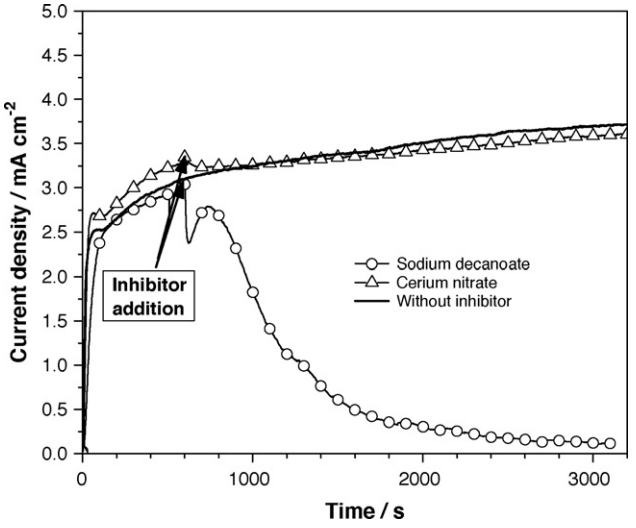

Fig. 11. Anodic current density versus time for the AA2024 polarized at −0.45 V/SCE in a solution containing 0.1 M Na_2SO_4 + 0.05 M NaCl with 0.025 M cerium nitrate or 0.025 M sodium decanoate injected into the solution after 600 s (pH 6).

This result confirms that the decanoate has protective properties by comparison with the cerium salts which have been largely described in the literature as potential candidates to replace chromates.

4. Conclusions

The mode of action of the sodium decanoate is to form a hydrophobic film on the AA2024 surface (shown by the high values of the contact angles) which strongly prevents attack of the passive layer by the chloride ions. Electrochemical impedance measurements showed that the efficiency was high over a large pH range (4–10). Local impedance maps on the Al/Cu couple showed that the decanoate was adsorbed on both metal surfaces thus limiting the galvanic coupling, responsible for the corrosion process. Finally, the molecule presents protective properties which constitute a significant point for an application in surface treatments of AA2024.

Acknowledgments

This work was carried out with the technical and financial support of the Défense Générale pour l'Armement and the European Aeronautic Defence and Space company.

The authors gratefully acknowledge Alain Lamure for his most valuable assistance in contact angle measurements.

References

[1] M. Kendig, A.J. Davenport, H.S. Isaacs, Corros. Sci. 34 (1993) 41.
[2] M. Kendig, S. Jeanjaquet, R. Addison, J. Waldrop, Surf. Coat. Technol. 140 (2001) 58.
[3] J. Zhao, L. Xia, A. Sehgal, D. Lu, R.L. McCreery, G.S. Frankel, Surf. Coat. Technol. 140 (2001) 51.
[4] L. Gancs, A.S. Besing, R. Bujak, A. Kolics, Z. Nemeth, A. Wieckowski, Electrochem. Solid State Lett. 5 (2002) B16.
[5] Z. Szklarska-Smialowska, Corros. Sci. 41 (1999) 1743.
[6] X. Zhao, G.S. Frankel, B. Zoofan, S. Rokhlin, Corrosion 59 (2003) 1012.
[7] X. Liu, G.S. Frankel, B. Zoofan, S. Rokhlin, Corros. Sci. 49 (2007) 139.
[8] I.L. Muller, J.R. Galvele, Corros. Sci. 17 (1977) 179.
[9] V. Guillaumin, G. Mankowski, Corros. Sci. 41 (1998) 421.
[10] W. Zhang, G.S. Frankel, Electrochim. Acta 48 (2003) 1193.
[11] C. Blanc, S. Gastaud, G. Mankowski, J. Electrochem. Soc. 150 (2003) B396.
[12] P. Schmutz, G.S. Frankel, J. Electrochem. Soc. 145 (1998) 2295.
[13] R.G. Buccheit, M.A. Martinez, L.P. Montes, J. Electrochem. Soc. 147 (2000) 119.
[14] R.G. Buchheit, L.P. Montes, M.A. Martinez, J. Michael, P.F. Hlava, J. Electrochem. Soc. 146 (1999) 4424.
[15] N. Birbilis, R.G. Buchheit, J. Electrochem. Soc. 152 (2005) B140.
[16] C. Blanc, A. Freulon, M.C. Lafont, Y. Kihn, G. Mankowski, Corros. Sci. 48 (2006) 3838.
[17] Y. Yoon, R.G. Buchheit, J. Electrochem. Soc. 153 (2006) B151.
[18] B. Hinton, N. Ryan, D. Arnott, P. Trathen, L. Wilson, B. Williams, Corrosion Australasia 10 (1985) 12.
[19] D. Arnott, B. Hinton, N. Ryan, Corrosion 45 (1989) 12.
[20] F. Mansfeld, S. Lin, S. Kim, H. Shih, Corrosion 45 (1989) 615.
[21] A. Davenport, H. Isaacs, M. Kendig, Corros. Sci. 32 (1991) 653.
[22] M. Bethencourt, F. Botana, J. Calvino, M. Marcos, M. Rodriguez-Chacon, Corros. Sci. 40 (1998) 1803.
[23] A.J. Aldykiewicz, H.S. Isaacs, A.J. Davenport, J. Electrochem. Soc. 142 (1995) 3342.
[24] A. Aballe, M. Bethencourt, F. Botana, M. Marcos, J. Alloys Compd. 323–324 (2001) 855.
[25] C. Casenave, N. Pébère, F. Dabosi, Mater. Sci. Forum 192–194 (1995) 599.
[26] M. Zheludkevich, K. Yasakau, S. Poznyak, M. Ferreira, Corros. Sci. 47 (2005) 3368.
[27] G. Boisier, A. Lamure, N. Pébère, N. Portail, M. Villatte, Surf. Coat. Technol. 203 (2009) 3420.
[28] C. Rapin, A. D'Huysser, J.P. Labbe, L. Gengembre, P. Steinmetz, Rev. Metall. 93 (1996) 719.
[29] E. Rocca, J. Steinmetz, Corros. Sci. 43 (2001) 891.
[30] A. Mercer, in: N.S. Ferrara, V. Sez (Eds.), Proceedings of the 5th European Symposium on Corrosion Inhibitors (5 SEIC), Ann. Univ. Suppl. N. 2, 1980, p. 563.
[31] G. Hefter, N. North, S. Tan, Corrosion 53 (1997) 657.
[32] U. Rammelt, S. Köhler, G. Reinhard, Electrochim. Acta 53 (2008) 6968.
[33] I. Raspini, Corrosion 49 (1993) 821.
[34] D. Daloz, C. Rapin, P. Steinmetz, G. Michot, Corrosion 54 (1998) 444.

[35] E. McCafferty, J.P. Wightman, J. Colloid Interface Sci. 194 (1997) 344.
[36] E. McCafferty, Corros. Sci. 45 (2003) 1421.
[37] J.-B. Jorcin, C. Blanc, N. Pébère, B. Tribollet, V. Vivier, J. Electrochem. Soc. 155 (2008) C46.
[38] G. Baril, C. Blanc, M. Keddam, N. Pébère, J. Electrochem. Soc. 150 (2003) B488.
[39] J.-B. Jorcin, E. Aragon, C. Merlatti, N. Pébère, Corros. Sci. 48 (2006) 1779.
[40] J.-B. Jorcin, M.E. Orazem, N. Pébère, B. Tribollet, Electrochim. Acta 51 (2006) 1473.
[41] L. Beaunier, I. Epelboin, J.C. Lestrade, H. Takenouti, Surf. Technol. 4 (1976) 237.
[42] K. Bonnel, C. Le Pen, N. Pébère, Electrochim. Acta 44 (1999) 4259.
[43] G.P. Shulman, A.J. Bauman, Met. Finish. 93 (1995) 16.
[44] C. Breslin, G. Treacy, W. Carroll, Corros. Sci. 36 (1994) 1143.